



**HAL**  
open science

## Interfacial hydrogen incorporation in epitaxial silicon for layer transfer

Junyang An, Zhen Zheng, Ruilin Gong, Thi Bao Tran Nguyen, Haeyeon Jun, Marta Chrostowki, Jean-Luc Maurice, Wanghua Chen, Pere Roca I Cabarrocas

► **To cite this version:**

Junyang An, Zhen Zheng, Ruilin Gong, Thi Bao Tran Nguyen, Haeyeon Jun, et al.. Interfacial hydrogen incorporation in epitaxial silicon for layer transfer. *Applied Surface Science*, 2020, 518, pp.146057. 10.1016/j.apsusc.2020.146057 . hal-02988828

**HAL Id: hal-02988828**

**<https://hal.science/hal-02988828>**

Submitted on 20 Nov 2020

**HAL** is a multi-disciplinary open access archive for the deposit and dissemination of scientific research documents, whether they are published or not. The documents may come from teaching and research institutions in France or abroad, or from public or private research centers.

L'archive ouverte pluridisciplinaire **HAL**, est destinée au dépôt et à la diffusion de documents scientifiques de niveau recherche, publiés ou non, émanant des établissements d'enseignement et de recherche français ou étrangers, des laboratoires publics ou privés.

# Interfacial hydrogen incorporation in epitaxial silicon for layer transfer

Junyang An<sup>1</sup>, Zhen Zheng<sup>1</sup>, Ruilin Gong<sup>1</sup>, Thi Bao Tran Nguyen<sup>2</sup>,  
HaeYeon Jun<sup>2</sup>, Marta Chrostowki<sup>2,3</sup>, Jean-Luc Maurice<sup>2</sup>, Wanghua Chen<sup>1,2\*</sup>  
and Pere Roca i Cabarrocas<sup>2\*</sup>

<sup>1</sup>*School of Physical Science and Technology, Ningbo University, Ningbo, 315211, P.R. China*

<sup>2</sup>*LPICM, CNRS, Ecole Polytechnique, Institut Polytechnique de Paris, Palaiseau 91128, France*

<sup>3</sup>*TOTAL S.A. Courbevoie 92069, France*

\*Email: [wanghua.chen@polytechnique.edu](mailto:wanghua.chen@polytechnique.edu);

[pere.roca@polytechnique.edu](mailto:pere.roca@polytechnique.edu);

## Abstract

*Recently, epitaxial Si layers have attracted strong attention, particularly in photovoltaics. This successful application depends mainly on the easiness of their transfer to a foreign carrier substrate. Therefore, developing a simple and efficient method to realize the transfer is a key issue. A most delicate point is the lift-off of the epitaxial layer from its parent substrate. In this work, we present a method to weaken the interface based on hydrogen incorporation. We have been able to control the hydrogen content at the interface between the crystalline silicon substrate and the epitaxial films by changing the epitaxial growth conditions. Several bonding techniques have been tested and epitaxial Si films have been*

*transferred successfully via anodic bonding. A hydrogen-assisted transferring mechanism is presented.*

Key words: Hydrogen; Epitaxial Si; Porosity; Layer transfer

## **1. Introduction**

Crystalline silicon (c-Si) thin films have many applications including photovoltaics[1-5] and flexible electronics.[6, 7] However, in the case of solar cell applications, one of the limiting factors is the cost of c-Si material itself, which can be reduced by decreasing the thickness of the c-Si absorber.[8, 9] Many techniques have been developed to produce c-Si thin films via “bottom-up”[9-12] and “top-down” approaches. [1, 3] Among these fabrication techniques, epitaxial growth has proven to be the most appropriate way to produce ultrathin monocrystalline films, since it enables the perfect control of the films thickness and their doping. In addition, when performed at low temperature (<200 °C) by using radio-frequency plasma-enhanced chemical vapor deposition (RF-PECVD),[11, 13-16] epitaxy is a low-cost process.

Whatever the applications and fabrication techniques, transferring the c-Si thin film to a foreign carrier substrate such as glass is mandatory in order to allow handling of fragile free-standing c-Si thin films. Different transfer methods have been proposed. For example, stress-induced techniques including SLIM cut;[17] and controlled spalling;[18] etching-enabled techniques such as macroporous Si[19] and sacrificial films;[20] implantation-induced techniques such as Smart-Cut process [21] as well as sintered porous-based techniques such as epifree process [3, 22] and porous Si.[23, 24] A detailed review of layer transfer techniques can be found in the literature.[9] Among them, two main techniques are commonly used. The first one is the Smart-Cut process.[21] This is a cleavage approach which is obtained by hydrogen ion implantation to create an in-depth fragile zone. However, a

high temperature annealing ( $> 600\text{ }^{\circ}\text{C}$ ) and a high-dose hydrogen ion implantation ( $1\times 10^{17}\text{ cm}^{-2}$ ) causing damage to the c-Si material are required to detach the c-Si thin film. The second technique is based on the use of porous silicon films: at least two regions with different porosity are created beneath the substrate surface by electrochemical etching in HF solutions before epitaxy.[25] The drawback of this technique is that it requires high temperature ( $> 1100\text{ }^{\circ}\text{C}$ ) sintering in hydrogen ambient.[24] Therefore, developing a detach/transfer method, which is fast, avoids the introduction of implantation-induced damage, and operates at low temperature (below  $300\text{ }^{\circ}\text{C}$ ), would reduce the thermal budget and processing cost.

In this work, we develop a method based on controlling the interface hydrogen content during the initial stages of epitaxy in a PECVD reactor, where a change of plasma deposition conditions is applied. We tested several bonding techniques and materials including silicone, polyimide, high temperature glue, and anodic bonding to study the transferring procedure. Various techniques such as spectroscopic ellipsometry, Raman spectroscopy, high-resolution transmission electron microscopy (HRTEM) and atomic force microscopy (AFM) are used to characterize the epitaxial interface. The pore formation mechanism is discussed.

## **2. Experiments**

Let us describe the standard transfer process, starting from the parent wafer and ending with a transferred c-Si thin film, as illustrate in Figure 1. Step 1 (Figure 1 (a)): preparation of a parent semiconductor substrate. This consists of removing the native oxide and surface contaminants, via two kinds of cleaning methods: i) standard HF-based chemical solutions (5 % HF, 30 seconds ) and ii) fluorine-based plasmas such as  $\text{SiF}_4$ [26]. The parent wafer is then loaded into a PECVD reactor. Here, a semi-industrial PECVD reactor (MVSystems Cluster tools) is used. Step 2 (Figure 1 (b)): substrate surface engineering to produce a fragile

interface. In this work, the interface engineering is realized by depositing porous epitaxial Si thin films using PECVD. Step 3 (Figure 1 (c)): epitaxial growth of a Si thin film using PECVD. The epitaxial growth is realized by using SiH<sub>4</sub> and H<sub>2</sub> as precursor and carrier gases, respectively. Step 4 (Figure 1 (d)): bonding the epitaxial films to a foreign substrate for transfer, for example, directly to glass at 250 °C and applying 1000 Volts for 10 min via anodic bonding. Step 5 (Figure 1 (e)): detaching the c-Si thin film from the parent wafer by applying a thermal annealing and mechanical force. Note that, in the case of solar cell fabrication, a junction forming layer such as doped hydrogenated amorphous Si (a-Si:H) and a back reflector layer/back contact layer such as Al will be deposited on the epitaxial Si layer before bonding it to glass. For the reference/standard epitaxial sample, the epi-PECVD film is grown directly on a cleaned parent Si wafer. In order to optimize interface engineering for facile detachment, different ultrathin layers are deposited on the c-Si substrate prior to the proper epitaxial growth.

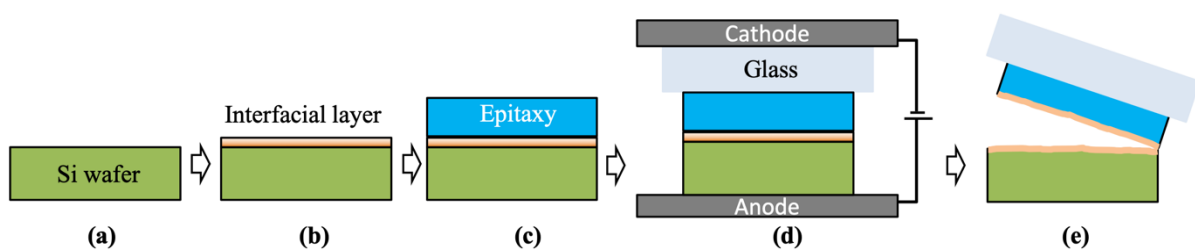


Figure 1. Schematic illustration of a standard process to transfer a c-Si thin film. (a) Preparation of a native oxide free parent Si wafer to serve as a seed for the epitaxial growth. (b) Interface engineering of parent Si substrate prior to epitaxial growth. (c) Epitaxial growth on the dedicated engineered surface. (d) Bonding to a foreign low-cost substrate such as glass via a bonding technique, for example, anodic bonding (250 °C; 1000 Volts; 10 min). (e) Detaching the ultra-thin film by annealing and applying a mechanical force. The parent wafer can be reused for the epitaxy of following batch.

### 3. Results

Figure 2 shows some characteristics of as-deposited epitaxial PECVD (epi-PECVD) Si thin films with and without interfacial layers. The results of spectroscopic ellipsometry (HORIBA Uvisel 2) measurements on six samples are presented in Figure 2 (a) and (b). The detailed epitaxial growth conditions are provided in Table 1. Briefly, sample A: standard reference epitaxy; sample B: single layer interface (type I); sample C: single layer interface (type II); sample D: bilayer interface (type I+II); sample E: bilayer interface (type I+II longer deposition time); sample F: bilayer interface (type I+II shorter deposition time). Note that the deposition time for sample B and C are adapted to keep their layer thicknesses the same. Insets in Figure 2 (a) and (b) show a zoom of low energy and high energy parts, respectively. At low energy, the amplitude of the imaginary part of the pseudo-dielectric function  $\varepsilon_i$  oscillations is characteristic of the interface porosity between epi-PECVD and c-Si substrate. At high energy range (3.4-3.5 eV), the amplitude of  $\varepsilon_i$  represents the crystalline quality. In terms of layer transfer, samples with higher interface porosity (higher amplitude at low energy part) while keeping good crystalline quality (higher amplitude at high energy part) are favored. By combining Figure 2 (a) and (b), we can see that such a compromise is detected by ellipsometry for the sample D (blue squares) grown with bilayer interface, as testified by the higher amplitude of the oscillations in the low energy range, compared to the reference epitaxy (black circles) and the high amplitude of  $\varepsilon_i$  at 3.45 eV, revealing a high crystalline quality. To check the crystalline quality of the epitaxial layers with different interface configuration, high resolution XRD was used as shown in Figure 2 (c). Similar dependence of epitaxy quality on interface process conditions can be observed as obtained from the ellipsometry data (Figure 2 (a)). A better crystalline quality of epitaxy in sample A and sample D can be observed in Figure 2 (c) showing a narrower full width at half maximum

(FWHM). The very large FWHM values of samples B and C indicates that the crystalline lattice in the epitaxial layers is distorted.

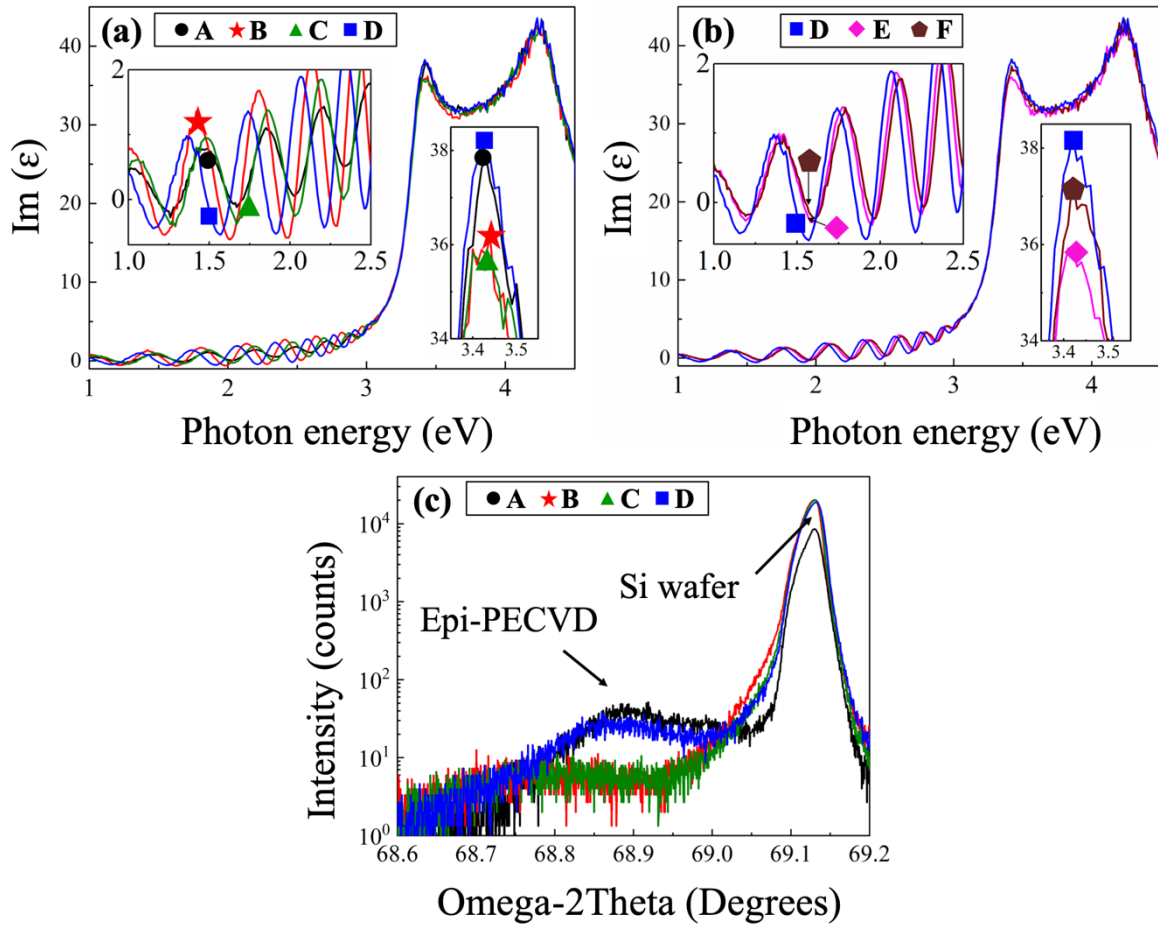


Figure 2. (a) Spectroscopic ellipsometry data of the imaginary part of the pseudo-dielectric function  $\epsilon_i$  of several Si epitaxial films with different interface process conditions for (a) samples A, B, C, D and (b) samples D, E, F. Inset showing the zooming of low energy and high energy parts, respectively. (c) High resolution XRD  $\omega$ - $2\theta$  scan data of Si epitaxy with different interface design of sample A, B, C and D.

Table 1. Detailed growth conditions for different epitaxial layers. Note that bulk epitaxial growth conditions are kept constant and only interface material process conditions are changed.

<b>Samples</b>	<b>Epitaxial region</b>	<b>H<sub>2</sub> (SCCM)</b>	<b>SiH<sub>4</sub> (SCCM)</b>	<b>Pressure (Torr)</b>	<b>Power (W)</b>	<b>Time (seconds)</b>
<b>A</b>	Bulk	200	4	2.3	20	1800
<b>B</b>	Interface	200	2	1.8	10	250
	Bulk	200	4	2.3	20	1800
<b>C</b>	Interface	200	1	1.7	5	450
	Bulk	200	4	2.3	20	1800
<b>D</b>	Bilayer interface	200	2	1.8	10	60
		200	1	1.7	5	60
	Bulk	200	4	2.3	20	1800
<b>E</b>	Bilayer interface	200	2	1.8	10	90
		200	1	1.7	5	90
	Bulk	200	4	2.3	20	1800
<b>F</b>	Bilayer interface	200	2	1.8	10	30
		200	1	1.7	5	30
	Bulk	200	4	2.3	20	1800

Once we have grown Si epitaxy layer with a porous interface, we can transfer them via bonding and lift-off. Since the typical thickness of epi-PECVD is below 10  $\mu\text{m}$ , a free-standing epi-PECVD would be rather difficult to manipulate and therefore its bonding to a foreign substrate such as glass is highly desirable. The key point for a successful transfer of epi-PECVD is to find a bonding technique compatible with our interface weakening method, based on hydrogen incorporation. Here, we tested different bonding techniques and materials

including silicone, polyimide, high temperature glue, and anodic bonding, to study their effects on epitaxy lift-off processes. A standard epitaxial layer (sample A) without intermediate layer of accumulated hydrogen is used as a reference. The transfer results are summarized in Table 2. The annealing process (200 °C for 10 minutes) is applied for each bonding technique before detaching the epi-PECVD thin film. As far as the standard epitaxy is concerned, we can see from Table 2 that the lift-off process is not OK whatever the bonding technique. For silicone, the bonding between epitaxial layer and the glass substrate before lift-off is OK. However, bonding loss between epitaxial layer and glass substrate occurs after annealing at 200 °C. In the case of polyimide, the lift-off process failed due to the loss of bonding between epitaxial layer and glass substrate during detachment. The high temperature glue formed bubbles during annealing and only tiny regions in the range of millimeter square could be detached. We found that the anodic bonding is the most successful technique for the transferring of epi-PECVD. In this case, the samples with epitaxial layers are put in contact with glass (corning 7740: Pyrex containing alkaline elements) under anodic bonding conditions (250 °C, 1000 V, 10 min). The glass side is connected to the cathode heating chuck. Note that, for the standard case, no detachment of epi-PECVD occurs at 500 °C for 10 min, even when the parent wafer was broken during lift-off process. Once samples properly bonded to glass via anodic bonding, they were heated at 300 °C in air for 5 min. Meanwhile, the lift-off of epitaxial thin film is performed, which is realized by applying a mechanical force at the glass/c-Si interface with a tweezer which leads to a crack initiation and propagation at the c-Si/epitaxy interface.

Table 2. Test of epitaxy transfer process (bonding and lift-off) with different bonding techniques.

<b>Sample</b>	<b>Description</b>	<b>Silicone</b>	<b>Polyimide</b>	<b>High temperature glue</b>	<b>Anodic bonding</b>
<b>A</b>	<b>Standard epitaxy</b>	Not OK	Not OK	Not OK	Not OK

<b>D</b>	<b>Epitaxy with hydrogen incorporation at interface</b>	OK for bonding, lift-off failed	OK for bonding, lift-off failed	OK for tiny region (mm <sup>2</sup> )	OK
----------	---	---------------------------------	---------------------------------	---------------------------------------	----

TEM was used in order to study the influence of anodic bonding on the microstructure of the epitaxial layers. The corresponding results are shown in Figure 3. for sample A without hydrogen incorporation, we observe no qualitative difference before (sample A) and after (sample A') anodic bonding (Figure 3 (a) and (b)) but, for sample D with interfacial hydrogen incorporation, there is difference before (sample D) and after (sample D') anodic bonding. Sample A has a less defective region at the top surface which is about 50 nm deep as it can be seen from Figure 3 (a), while the depletion at the top surface of sample D is much shallower (Figure 3 (c)). By comparing epitaxy with interfacial hydrogen incorporation of sample D (Figure 3 (c)) and D' and (Figure 3 (d)), we observe the formation of columnar structures in sample D'. This gathering of defects in the form of columns also corresponds to a global defect-density decrease (see below). There could be something like the beginning of a "polygonization", which happens in metallurgy when deformation-induced dislocations group to form sub-grain boundaries. [27]

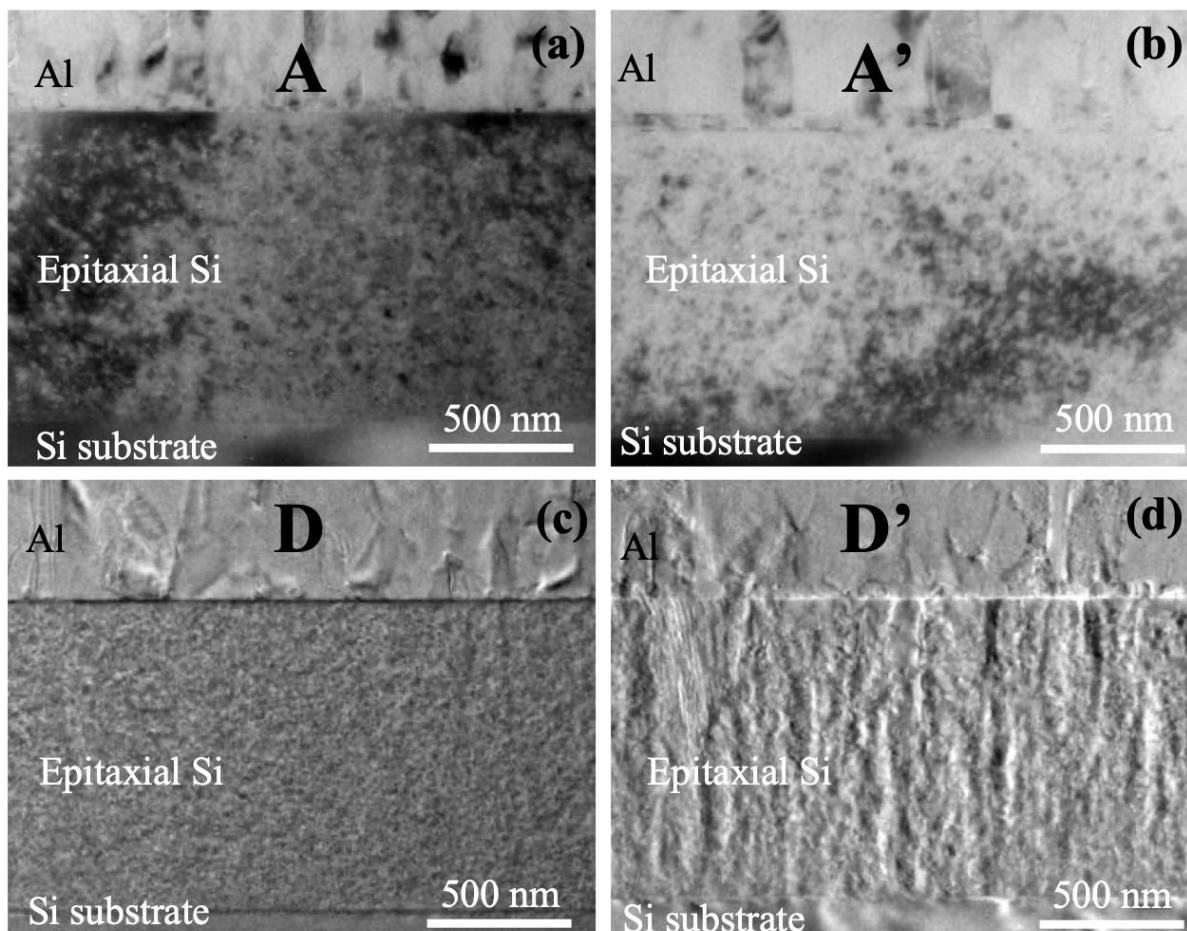


Figure 3. TEM characterization of epitaxy interface quality under different conditions. Reference Si epitaxy (a) before (sample A) and (b) after (sample A') anodic bonding. Epitaxy with interfacial hydrogen incorporation (c) before (sample D) and (d) after (sample D') anodic bonding.

Let us now quantitatively measure the defects in epitaxial Si layer with the help of TEM characterization. The principle of defect measurement in TEM is illustrated in Figure 4. First of all, a hole is drilled in thin foil (TEM lamella) with the e-beam with a  $30^\circ$  tilt as shown in Figure 4 (a). Then, the foil is tilted back to  $0^\circ$  for observation (Figure 4 (b)). We have a relation of  $t=d/\tan 30^\circ$ , where  $t$  is the foil thickness and  $d$  is the apparent length of the

drilled hole as illustrated in Figure 4 (c) and (d). The raw measurement of defect density ( $\mu\text{m}^{-2}$ ) is counted directly from the TEM images, for example, TEM image in Figure 4 (c). Then, the volume density ( $\mu\text{m}^{-3}$ ) can be obtained by dividing the raw measurement with foil thickness  $t$ . The area density ( $\text{cm}^{-2}$ ) equals to (volume density ( $\text{cm}^{-3}$ ))<sup>2/3</sup>. The raw measurement data is collected from an average of 3 to 4 measurements. Based on this protocol, the platelet defect density of samples A, A', D and D' can be calculated. The corresponding data is presented in Table 3. We can conclude from Table 3 that the defect density near the surface is lower than at the interface for all of these four samples. The higher defect density at interface is due to the slight lattice difference between c-Si substrate and c-Si:H epitaxial layer [12]. Note that the average error on the TEM density measurements is about  $0.5 \times 10^{11} \text{ cm}^{-2}$ , except for sample D' where it is about  $0.2 \times 10^{11} \text{ cm}^{-2}$ . By comparing samples A and A' (without interface treatment), we can see that the standard epitaxial Si layer has a roughly constant defect density. The interfacial platelet defect density is further increased to  $2 \times 10^{11} \text{ cm}^{-2}$  in sample D of epitaxial Si with a gradient interface. Interestingly, this value has been greatly decreased to  $0.7 \times 10^{11} \text{ cm}^{-2}$  for sample D' after anodic bonding. Moreover, the defect density near surface of sample D' has been also reduced to  $0.7 \times 10^{11} \text{ cm}^{-2}$ , which is a value much lower as compared to other epitaxial samples at the same region near epitaxy surface. We can also observe the presence of hydrogen platelet defects in Figure 4 (d). However, such kind of platelets are aligned in sample D' after anodic bonding. Because of alignment, the coalescence of platelets occurs. As a result, the platelet defect density is decreased both near surface and at interface. The reason of coalescence of hydrogen platelets will be presented in the discussion part afterward.

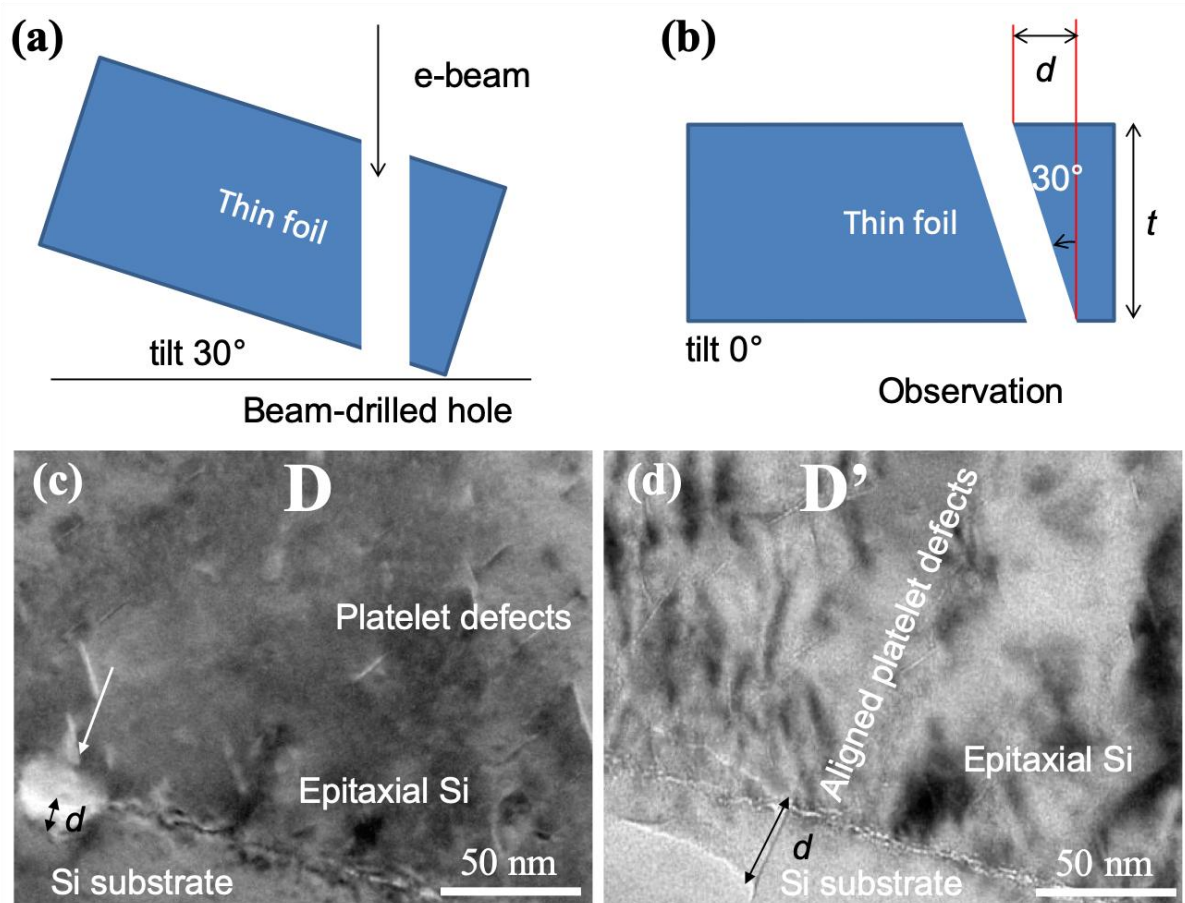


Figure 4. Schematic illustration of the method for defect measurement using TEM images. (a) Tilt at  $30^\circ$  to drill a hole in thin foil with e-beam then (b), tilt at  $0^\circ$  for observation. TEM cross-section of epitaxial Si of sample D (c) and sample D' (d). The white arrow in (c) indicates the hole for foil thickness measurement.

Table 3. Platelet defect density of 4 different epitaxial Si layers near surface and at interface.

Samples	Regions	Defect density ( $10^{11} \text{ cm}^{-2}$ )
A	Surface	0.92
	Interface	1.05
A'	Surface	1.1
	Interface	1.5
D	Surface	1.4
	Interface	2.0
D'	Surface	0.66
	Interface	0.68

To characterize the interfacial structure, the microstructural evolution of sample A to A' (standard epitaxy) as well as that of sample D to D' (bi-layer epitaxy with hydrogen incorporation at interface) is investigated by HRTEM. Figure 5 (a) and (b) show the HRTEM characterization of samples A and A' (as-deposited and after anodic bonding cases), respectively. The corresponding interface HRTEM images are presented in the insets of Figure 5 (a) and (b). Interestingly, we can see that the interface between epitaxy and substrate is almost invisible. The presence of hydrogen platelets can be observed, which is typical for PECVD-grown epitaxial layers.[16] We can observe in Figure 5 (c) as well as its HRTEM image in the inset that there is a discontinuous interface contrast or porosity in sample D, for which more hydrogen atoms were incorporated at the interface. The width of the interface is estimated to be one monolayer. Interestingly, we can see that the width of the interface increases to ~ 1 nm after anodic bonding as shown in Figure 5 (d). As evidenced in the inset of Figure 5 (d), defects are observed at interface, which indicates that the interface becomes amorphous or has a low atomic density. In other words, it becomes fragile.

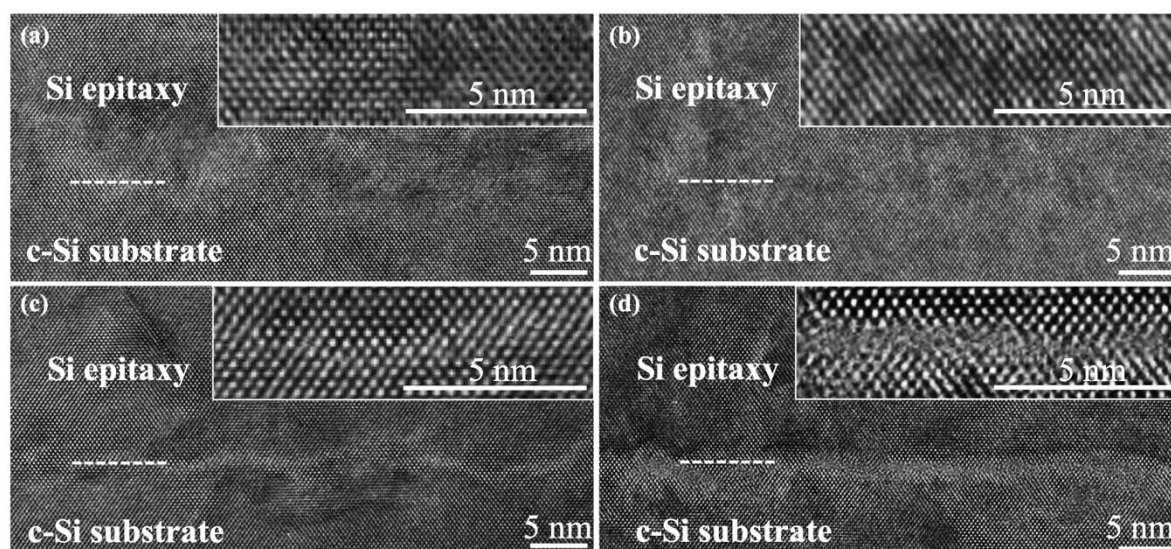


Figure 5. High resolution TEM characterization of epitaxial Si/c-Si interface quality under different conditions. (a) As-deposited reference epitaxy (sample A). (b) Reference epitaxy

after anodic bonding (sample A'). (c) As-deposited epitaxy with hydrogen incorporation at interface (sample D). (d) Epitaxy with hydrogen incorporation at interface after anodic bonding (sample D'). Insets in (a), (b), (c) and (d) show the corresponding HRTEM images at the interface between epitaxy and substrate.

Raman spectroscopy (532 nm excitation laser) was used to investigate the incorporation of hydrogen for three epitaxial layers including samples A, D and D'. The detailed data are presented in Figure 6. Similar crystallinity of samples A and D is evidenced as shown in Figure 6 (a), where the corresponding full width at half maximum (FWHM) values are 8.1 and 8.3, respectively. However, epitaxy after anodic bonding (sample D') exhibits a slightly higher value of FWHM of 10.1 indicating that some degradation of epitaxial quality occurs during anodic bonding. Combining Figure 6 (b) and (c), it can be observed that neither Si-H nor H-H bonding appear in epitaxial Si after anodic bonding (sample D'). This indicates that H atoms and molecules can be desorbed at a temperature as low as 250 °C under 1000 Volts in 10 min. In pure thermal annealing conditions, H can only be desorbed around 300 °C for the intrinsic epitaxial Si [28]. The much lower desorption temperature must be related to the high voltage (1000 Volts) applied for anodic bonding. The epitaxial layer was in contact with the cathode during anodic bonding and it is expected that hydrogen (H+) in epitaxial Si will move towards the cathode, which will consequently desorb hydrogen from epitaxial layer.

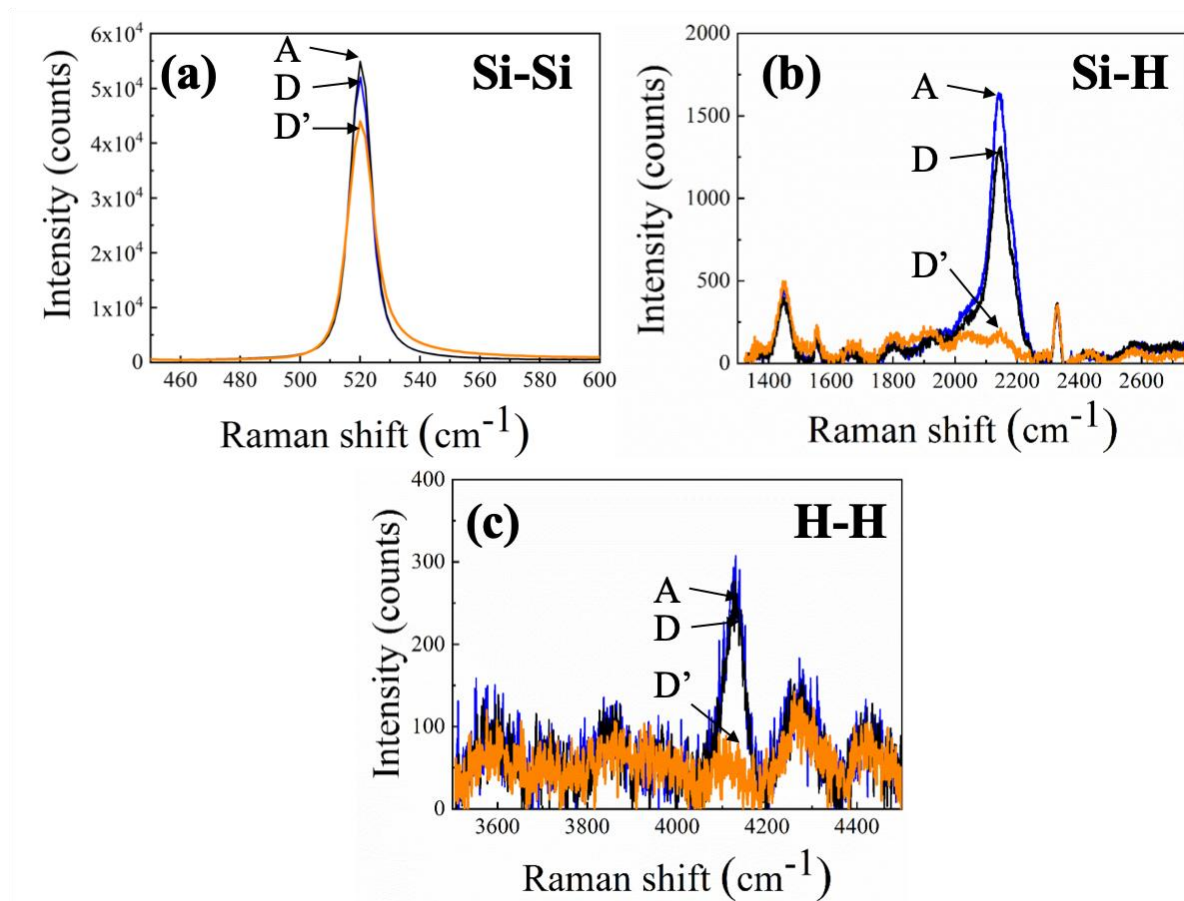


Figure 6. Raman spectra of three epitaxial samples (A, D, D') at different shift range with (a), (b) and (c) corresponding to Si-Si bonds (520 cm<sup>-1</sup>), Si-H bonds (2100 cm<sup>-1</sup>) and H-H bonds (4100 cm<sup>-1</sup>), respectively.

The morphology of epitaxial Si surface (sample D') is investigated with the help of AFM (Asylum research, Oxford instruments). AFM tips (AC240TM) from Olympus were used, which has a doped Si cantilever and a Pt coating. Two types of surface of epitaxial Si were characterized including the top surface of epitaxy Si before bonded to glass and the detached surface after transferring, which corresponds to the interface before transferring. The corresponding results are shown in Figure 7. Figure 7 (a) presents the AFM characterization of the top surface of Si epitaxial layer before it's bonded to glass. From Figure 7 (a), we can see that the top surface of epitaxial Si layer exhibits some humps and holes at nanoscale. The root mean square (RMS) value can be calculated to be 1.2 nm. Figure 7 (c) shows the

corresponding AFM image of the detached surface of the epitaxial Si after being bonded to glass. As in the case of top surface of epitaxial Si layer, we can also detect several humps and holes. The corresponding RMS value is the same as in the top surface of 1.2 nm.

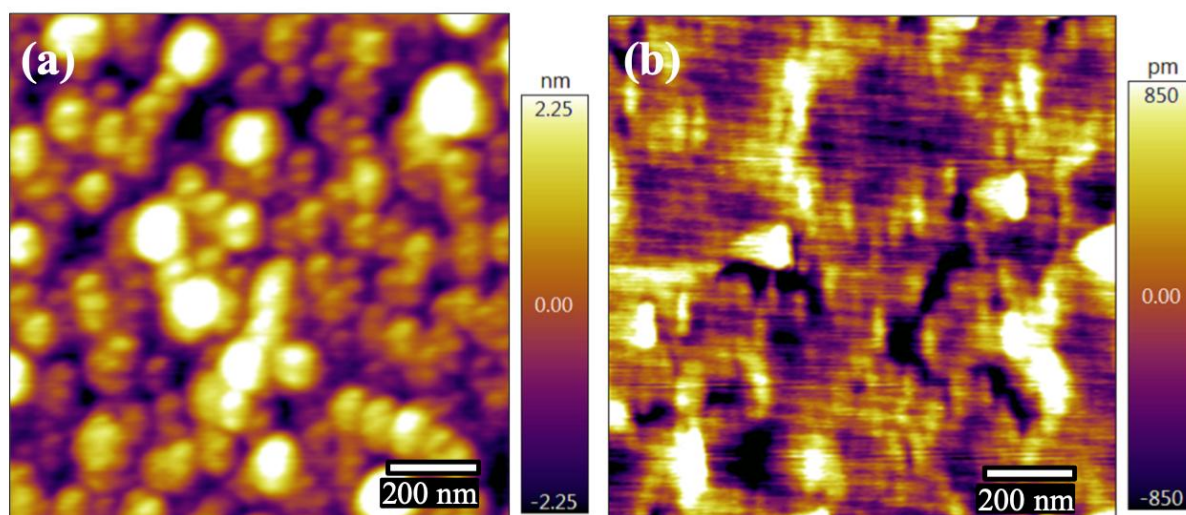


Figure 7. AFM mapping of epitaxial Si layers. (a) and (b) present the AFM characterization of top surface of Si epitaxial layer before being bonded to glass and detached surface of the epitaxial Si layer bonded to glass, respectively.

#### 4. Discussion

The mechanism of pore formation via interfacial hydrogen incorporation can be discussed as follows. Based on our characterization results above, hydrogen atoms are considered to be the dominant element causing the detachment of the Si epitaxial layer. Therefore, we considered the evolution of hydrogen atoms in three steps: epitaxy, anodic bonding and annealing. During epitaxial growth, the bilayer interface enhances the incorporation of hydrogen atoms during film growth. This can be attributed to the higher disorder in these layers as compared to monocrystalline Si. Compared to the introduction of H atoms via ion implantation in a Smart-Cut process,[21] here H atoms are incorporated during the epitaxial growth. During anodic bonding at 250 °C, it is reported that hydrogen ions ( $H^+$ ) in glass move in the same direction as  $Na^+$  towards the cathode [29, 30]. Therefore, we can

expect that hydrogen in the epitaxial Si layer moves also towards the cathode, away from Si wafer. This can be evidenced by the Raman data in Figure 6 (a) and (c) showing the disappearing of Si-H and H-H peak after anodic bonding. By comparing HRTEM images in Figure 5 (c) and (d), we also observed that the interfacial defective region has been widened and smoothed after anodic bonding due to the exodifusion of hydrogen in epitaxial Si layer. The micro cavities formed during anodic bonding because of H<sub>2</sub> molecule evolution will be further expanded with a tweezer-induced mechanical force upon annealing at 300 °C. Therefore, a coalescence of these micro cavities occurs leading to the peel-off of epitaxial Si layer.

## **5. Conclusion**

In summary, we have developed an interface modification method based on the deposition of a bilayer epitaxial Si to produce a fragile thin film interface for layer transfer. By adding a thin bilayer prior to the bulk epitaxial growth, the interface porosity can be greatly enhanced as evidenced by ellipsometry. The accumulation of H atoms at the interface helps to fragilize the interface upon annealing. Anodic bonding is found to be compatible with our transfer method of producing a fragile interface based on hydrogen incorporation. With the help of HRTEM, we found that the micro cavities (porosity) are formed at the interface, which is most likely due to the exodifusion of hydrogen during anodic bonding.

## **Acknowledgement**

This project has been supported by European Union's Seventh Framework Programme PhotoNVoltaics under grant agreement No 309127 and French Government in the frame of the program of investment for the future (Programme d'Investissement d'Avenir - ANR-IEED-002-01 and TEMPOS Equipex – ANR-10-EQPX-50, pole NanoMAX).

## References

- [1] G.P. Willeke, Thin crystalline silicon solar cells, *Solar Energy Materials and Solar Cells*, 72 (2002) 191-200.
- [2] A. Gaucher, A. Cattoni, C. Dupuis, W. Chen, R. Cariou, M. Foldyna, L.c. Lalouat, E. Drouard, C. Seassal, P. Roca i Cabarrocas, S. Collin, Ultrathin Epitaxial Silicon Solar Cells with Inverted Nanopyramid Arrays for Efficient Light Trapping, *Nano Letters*, 16 (2016) 5358-5364.
- [3] V. Depauw, C. Trompoukis, I. Massiot, W. Chen, A. Dmitriev, P. Roca i Cabarrocas, I. Gordon, J. Poortmans, Sunlight-thin nanophotonic monocrystalline silicon solar cells, *Nano Futures*, 1 (2017) 021001.
- [4] P. Pathi, A. Peer, R. Biswas, Nano-Photonic Structures for Light Trapping in Ultra-Thin Crystalline Silicon Solar Cells, *Nanomaterials*, 7 (2017).
- [5] H. Dai, L. Yang, S. He, < 50- $\mu\text{m}$  thin crystalline silicon heterojunction solar cells with dopant-free carrier-selective contacts, *Nano Energy*, 64 (2019) 103930.
- [6] Z. Ma, K. Zhang, J.-H. Seo, H. Zhou, L. Sun, H.-C. Yuan, G. Qin, H. Pang, W. Zhou, Fast Flexible Electronics Based on Printable Thin Mono-Crystalline Silicon, *ECS Transactions*, 34 (2011) 137-142.
- [7] H. Zhou, J.-H. Seo, D.M. Paskiewicz, Y. Zhu, G.K. Celler, P.M. Voyles, W. Zhou, M.G. Lagally, Z. Ma, Fast flexible electronics with strained silicon nanomembranes, *Scientific Reports*, 3 (2013) 1291.
- [8] C. Trompoukis, I. Abdo, R. Cariou, I. Cosme, W. Chen, O. Deparis, A. Dmitriev, E. Drouard, M. Foldyna, E.G. Caurel, I. Gordon, B. Heidari, A. Herman, L. Lalouat, K.-D. Lee, J. Liu, K. Lodewijks, F. Mandorlo, I. Massiot, A. Mayer, V. Mijkovic, J. Muller, R. Orobtcouk, G. Poulain, P. Prod'Homme, P. Roca i Cabarrocas, C. Seassal, J. Poortmans, R. Mertens, O.E. Daif, V. Depauw, Photonic nanostructures for advanced light trapping in thin crystalline silicon solar cells, *Physica Status Solidi A*, 212 (2015) 140-155.
- [9] H. Sivaramakrishnan Radhakrishnan, J. Cho, T. Bearda, J. Röth, V. Depauw, K. Van Nieuwenhuysen, I. Gordon, J. Szlufcik, J. Poortmans, Freestanding and supported processing of sub-70  $\mu\text{m}$  kerfless epitaxial Si and thinned Cz/FZ Si foils into solar cells: An overview of recent progress and challenges, *Solar Energy Materials and Solar Cells*, 203 (2019) 110108.
- [10] M. Breitwieser, F.D. Heinz, T. Rachow, M. Kasemann, S. Janz, W. Warta, M.C. Schubert, Process Control and Defect Analysis for Crystalline Silicon Thin Films for Photovoltaic Applications by the Means of Electrical and Spectroscopic Microcharacterization Tools, *IEEE Journal of Photovoltaics*, 4 (2014) 1275-1281.
- [11] W. Chen, R. Cariou, G. Hamon, R. Léal, J.-L. Maurice, P. Roca i Cabarrocas, Influence of deposition rate on the structural properties of plasma-enhanced CVD epitaxial silicon, *Scientific Reports*, 7 (2017) 43968.
- [12] W. Chen, G. Hamon, R. Léal, J.-L. Maurice, L. Largeau, P. Roca i Cabarrocas, Growth of Tetragonal Si via Plasma-Enhanced Epitaxy, *Crystal Growth & Design*, 17 (2017) 4265-4269.
- [13] M. Moreno, P. Roca i Cabarrocas, Ultra-thin crystalline silicon films produced by plasma assisted epitaxial growth on silicon wafers and their transfer to foreign substrates, *EPJ Photovoltaics*, 1 (2010) 6.
- [14] M. Labrune, X. Bril, G. Patriarche, L. Largeau, O. Mauguin, P. Roca i Cabarrocas, Epitaxial growth of silicon and germanium on (100)-oriented crystalline substrates by RF PECVD at 175 °C, *EPJ Photovoltaics*, 3 (2012) 30303.

- [15] B. Demaurex, R. Bartlome, J.P. Seif, J. Geissbühler, D.T.L. Alexander, Q. Jeangros, C. Ballif, S. De Wolf, Low-temperature plasma-deposited silicon epitaxial films: Growth and properties, *Journal of Applied Physics*, 116 (2014) 053519.
- [16] W. Chen, J.-L. Maurice, J.-C. Vanel, P. Roca i Cabarrocas, Powder free PECVD epitaxial silicon by plasma pulsing or increasing the growth temperature, *Journal of Physics D: Applied Physics*, 51 (2018) 235203.
- [17] P. Bellanger, P.-O. Bouchard, M. Bernacki, J. Serra, Room temperature thin foil SLIM-cut using an epoxy paste: experimental versus theoretical results, *Materials Research Express*, 2 (2015) 046203.
- [18] S.W. Bedell, D. Shahrjerdi, B. Hekmatshoar, K. Fogel, P.A. Lauro, J.A. Ott, N. Sosa, D. Sadana, Kerf-Less Removal of Si, Ge, and III–V Layers by Controlled Spalling to Enable Low-Cost PV Technologies, *IEEE Journal of Photovoltaics*, 2 (2012) 141-147.
- [19] R. Brendel, M. Ernst, Macroporous Si as an absorber for thin-film solar cells, *physica status solidi (RRL) – Rapid Research Letters*, 4 (2010) 40-42.
- [20] G. Hamon, N. Vaissiere, R. Cariou, R. Lachaume, J. Alvarez, W. Chen, J.-P. Kleider, J. Decobert, P. Roca i Cabarrocas, Plasma-enhanced chemical vapor deposition epitaxy of Si on GaAs for tunnel junction applications in tandem solar cells, *Journal of Photonics for Energy*, 7 (2017) 022504.
- [21] M. Bruel, B. Aspar, A.-J. Auberton-Hervé, Smart-Cut: A New Silicon On Insulator Material Technology Based on Hydrogen Implantation and Wafer Bonding\*1, *Japanese Journal of Applied Physics*, 36 (1997) 1636-1641.
- [22] V. Depauw, Y. Qiu, K. Van Nieuwenhuysen, I. Gordon, J. Poortmans, Epitaxy-free monocrystalline silicon thin film: first steps beyond proof-of-concept solar cells, *Progress in Photovoltaics: Research and Applications*, 19 (2011) 844–850.
- [23] K. Feldrapp, R. Horbelt, R. Auer, R. Brendel, Thin-film (25.5  $\mu\text{m}$ ) solar cells from layer transfer using porous silicon with 32.7 mA/cm<sup>2</sup> short-circuit current density, *Progress in Photovoltaics: Research and Applications*, 11 (2003) 105–112.
- [24] H. Sivaramakrishnan Radhakrishnan, R. Martini, V. Depauw, K. Van Nieuwenhuysen, T. Bearda, I. Gordon, J. Szlufcik, J. Poortmans, Kerfless layer-transfer of thin epitaxial silicon foils using novel multiple layer porous silicon stacks with near 100% detachment yield and large minority carrier diffusion lengths, *Solar Energy Materials and Solar Cells*, 135 (2015) 113-123.
- [25] B. Terheiden, Homoepitaxy on Porous Silicon, in: L. Canham (Ed.) *Handbook of Porous Silicon*, Springer International Publishing, 2014.
- [26] M. Moreno, M. Labrune, P. Roca i Cabarrocas, Dry fabrication process for heterojunction solar cells through in-situ plasma cleaning and passivation, *Solar Energy Materials and Solar Cells*, 94 (2010) 402-405.
- [27] G.E. Totten, *Steel Heat Treatment Handbook: Metallurgy and Technologies*, Taylor & Francis, 1 (2007).
- [28] M. Chrostowski, R. Peyronnet, W. Chen, N. Vaissiere, J. Alvarez, E. Drahi, P. Roca i Cabarrocas, Low temperature epitaxial growth of boron-doped silicon thin films, *AIP Conference Proceedings*, 1999 (2018) 070001.
- [29] T.M. McCrone, The Creation of an Anodic Bonding Device Setup and Characterization of the Bond Interface Through the use of the Plaza Test, Thesis, (2012) pp. 15.
- [30] W. Chen, V. Depauw, F. Haddad, J.-L. Maurice, P. Roca i Cabarrocas, Influence of anodic bonding on the surface passivation quality of crystalline silicon, *Solar Energy Materials and Solar Cells*, 157 (2016) 154-160.